Elastic differential cross section and critical point for positron-hydrogen collisions

Arijit Ghoshal[1] and Puspajit Mandal[2]
[1]*Department of Mathematics, Suri Vidyasagar College Suri 731 101 West Bengal, India*
[2]*Department of Mathematics, Visva-Bharati University Santiniketan 731 235 West Bengal, India*
(Received 22 April 2005; published 14 October 2005)

A detailed study is made of the elastic differential cross section in positron-hydrogen collisions using the accurate Schwinger variational results for partial waves up to $l=19$ of the preceding paper [Ghoshal and Mandal, Phys. Rev. A, **72**, 042709 (2005)]. Dramatic behavior of the differential cross section is evident in the surface plots, suggesting interference of partial-wave contributions at small and large scattering angles for the appearance of rich structure. It is found that the behavior of the critical point basically characterizes the nature of the differential cross section. Further interferences of the scattered waves for different angular momentum states produced by the interaction between the incoming positron and the target hydrogen atom determine such behavior and consequently build up the nature of the differential cross section. These findings reveal the remarkable fact that positron-hydrogen scattering almost does not occur in the direction around 87.3° at an incident energy of about 3.4 eV, corresponding to incident positron momentum of 0.5 atomic units.

DOI: 10.1103/PhysRevA.72.042710 PACS number(s): 34.80.Gs, 34.70.+e, 36.10.Dr

I. INTRODUCTION

In the preceding paper, paper I [1], the authors have applied the Schwinger variational method to investigate elastic positron-hydrogen collision. With the help of the correlated dipole-polarized basis, accurate results of the phase shifts have been reported for incident positron momentum in the range 0.1–3.5 atomic units (a.u.). These results are in conformity with the available theoretical calculations using both variational and nonvariational methods.

The theoretical study of differential cross section is of utmost importance in collision phenomena not only because the results of experiment are expressed by means of this quantity, but also because this quantity characterizes the collision process. The nature of the differential cross section is basically characterized by the behavior of the critical points. These points are defined to be those incident energies or scattering angles for which the differential cross section assumes its minimum value. A careful observation of the existence and behavior of the critical points unfolds some dramatic properties of the differential cross section in positron-hydrogen collisions.

In spite of having a vital role in determining the detailed nature of the differential cross section, the study of critical points has not drawn the serious attention of workers. One of the reasons for this seems to be that accurate results of the scattering parameters are limited to a few partial waves. However, using empirical relationships satisfied by the phase shifts, Wadhera *et al.* [2] predicted the existence of critical points for positron–rare-gas-atoms collisions with Ar, Kr, and Xe due to low-energy positron diffraction. An analysis by Buhring [3] in the case of electron-atom collisions has shown that elastically scattered electrons are fully polarized when the scattering angle and the incident energy correspond to the critical values. The origin of this polarization effect has been found to be the spin-orbit coupling which arises in a many-electron atomic system.

Of late, using accurate variational results Kar *et al.* [4] were able to demonstrate in an elegant way the existence and behavior of critical angles in elastic positron-hydrogen collision in the low-energy region with the help of surface plots.

In this paper our main objective is to make a detailed study of the elastic differential cross section for positron-hydrogen collisions using the accurate Schwinger variational results of the preceding paper [1]. Use of surface plots is made to have a concrete idea about the existence and behavior of the critical points which determine the nature of the differential cross section. In the process we give a detailed analysis of the occurrence of a primary minimum and secondary maximum in the differential cross section by displaying striking features in their structures.

The plan of the paper is as follows. In Sec. II we discuss our approach for obtaining the elastic differential cross section in positron-hydrogen collisions. Section III is devoted to the discussions of the results as obtained by the present calculations. Finally in Sec. IV we make our concluding remarks.

II. THEORY

The elastic differential cross section for positron-hydrogen scattering is obtained as

$$\frac{d\sigma}{d\Omega} = |f(\vec{k}_f,\vec{k}_i)|^2 \quad (\text{units of } a_0^2)$$
$$= |f_r(\vec{k}_f,\vec{k}_i)|^2 + |f_i(\vec{k}_f,\vec{k}_i)|^2 \quad (\text{units of } a_0^2), \qquad (1)$$

where $f_r(\vec{k}_f,\vec{k}_i)$ and $f_i(\vec{k}_f,\vec{k}_i)$ are, respectively, the real and imaginary parts of the scattering amplitude $f(\vec{k}_f,\vec{k}_i)$. In order to obtain convergence in the results, it is required to take a large number of partial-wave contributions into account. This is accomplished by making use of our accurate Schwinger variational results for a maximum of $L=19$ partial waves and approximating the next higher partial-wave amplitudes with the help of the effective-range formula of O'Malley *et al.* [5]. With this approximation $f_r(\vec{k}_f,\vec{k}_i)$ and $f_i(\vec{k}_f,\vec{k}_i)$ take the forms

TABLE I. The elastic differential cross section (a.u.) for incident positron momenta k_i=0.3–0.8 a.u.

Angle (deg)	k_i=0.3	k_i=0.4	k_i=0.5	k_i=0.6	k_i=0.7	k_i=0.8
120.0	0.056494	0.006418	0.066676	0.142749	0.220136	0.187286
122.0	0.050650	0.008418	0.071718	0.146113	0.219268	0.186308
124.0	0.045325	0.010556	0.076524	0.149083	0.217604	0.185114
126.0	0.040497	0.012805	0.081041	0.151645	0.215234	0.183617
128.0	0.036141	0.015147	0.085246	0.153761	0.212302	0.181820
130.0	0.032224	0.017567	0.089148	0.155394	0.208995	0.179816
132.0	0.028712	0.020053	0.092789	0.156527	0.205492	0.177753
134.0	0.025567	0.022589	0.096229	0.157185	0.201930	0.175787
136.0	0.022751	0.025155	0.099534	0.157437	0.198360	0.174029
138.0	0.020229	0.027721	0.102758	0.157390	0.194748	0.172509
140.0	0.017968	0.030254	0.105931	0.157163	0.190987	0.171171
142.0	0.015942	0.032715	0.109046	0.156861	0.186940	0.169892
144.0	0.014127	0.035070	0.112064	0.156548	0.182502	0.168522
146.0	0.012507	0.037288	0.114917	0.156232	0.177649	0.166940
148.0	0.011067	0.039351	0.117522	0.155868	0.172463	0.165091
150.0	0.009798	0.041256	0.119803	0.155370	0.167132	0.163009
152.0	0.008690	0.043015	0.121708	0.154645	0.161909	0.160804
154.0	0.007735	0.044654	0.123224	0.153631	0.157053	0.158625
156.0	0.006922	0.046209	0.124380	0.152325	0.152765	0.156611
158.0	0.006242	0.047721	0.125252	0.150799	0.149141	0.154838
160.0	0.005680	0.049225	0.125944	0.149197	0.146155	0.153298
162.0	0.005223	0.050748	0.126567	0.147708	0.143665	0.151895
164.0	0.004858	0.052302	0.127226	0.146527	0.141464	0.150478
166.0	0.004571	0.053876	0.127992	0.145809	0.139337	0.148891
168.0	0.004348	0.055441	0.128893	0.145635	0.137125	0.147036
170.0	0.004180	0.056946	0.129906	0.145986	0.134781	0.144916
172.0	0.004055	0.058323	0.130962	0.146743	0.132385	0.142652
174.0	0.003967	0.059500	0.131959	0.147706	0.130127	0.140466
176.0	0.003908	0.060404	0.132782	0.148635	0.128257	0.138632
178.0	0.003874	0.060973	0.133324	0.149302	0.127017	0.137407
180.0	0.003864	0.061168	0.133514	0.149544	0.126583	0.136976

$$f_r(\vec{k}_f,\vec{k}_i) = \frac{1}{k_i}\left(\sum_{l=0}^{L}(2l+1)f_r^{(v)}(k_f,k_i)P_l(\cos\theta) + \sum_{l=L+1}^{\infty}(2l+1)f^{(p)}(k_f,k_i)P_l(\cos\theta)\right), \quad (2)$$

and

$$f_i(\vec{k}_f,\vec{k}_i) = \frac{1}{k_i}\left(\sum_{l=0}^{L}(2l+1)f_i^{(v)}(k_f,k_i)P_l(\cos\theta)\right). \quad (3)$$

Here $P_l(\cos\theta)$ denotes the Legendre polynomial of the first kind of order l, θ is the scattering angle, $f_r^{(v)}(k_f,k_i)$ and $f^{(p)}(k_f,k_i)$ are, respectively, the real parts of the amplitudes obtained by using Schwinger's principle and the effective-range formula respectively, whereas $f_i^{(v)}(k_f,k_i)$ is the imaginary part of the variational amplitude.

That these values are highly reliable can be ascertained from the fact that total cross sections obtained by using any of the following formulas reproduce the same results:

$$\begin{aligned}\sigma &= \left(\frac{4}{k_i^2}\right)\sum_{l=0}^{L}(2l+1)\sin^2\delta_l \quad (\text{units of } \pi a_0^2)\\ &= 2\int_{-1}^{+1}\frac{d\sigma}{d\Omega}d(\cos\theta) \quad (\text{units of } \pi a_0^2)\\ &= \left(\frac{4}{k_i}\right)\mathrm{Im}\,f(0) \quad (\text{units of } \pi a_0^2) \quad (\text{optical theorem}).\end{aligned} \quad (4)$$

III. RESULTS AND DISCUSSION

We now present the nature of $d\sigma/d\Omega$ in some detail.

TABLE II. The critical angles θ_c(deg) along with the corresponding differential cross sections $(d\sigma/d\Omega)_c$(a.u.) in elastic positron-hydrogen collisions at incident energies $k_i \in [0.1, 3.5]$ a.u.. $x[-y]$ denotes $x \times 10^{-y}$.

k_i	θ_c	$(d\sigma/d\Omega)_c$	k_i	θ_c	$(d\sigma/d\Omega)_c$	k_i	θ_c	$(d\sigma/d\Omega)_c$
0.1	180.0	1.6216	1.3	28.3	0.0073	2.5	180.0	0.0032
0.2	180.0	0.2832	1.4	23.4	0.0074	2.6	172.0	0.0031
0.3	180.0	0.0039	1.5	19.6	0.0083	2.7	172.0	0.0026
0.4	108.7	0.0001	1.6	17.2	0.0086	2.8	180.0	0.0022
0.5	87.3	4.61[−5]	1.7	15.7	0.0088	2.9	173.0	0.0020
0.6	73.7	0.0004	1.8	180.0	0.0082	3.0	173.0	0.0018
0.7	65.8	0.0020	1.9	180.0	0.0075	3.1	180.0	0.0015
0.8	55.8	0.0055	2.0	172.0	0.0067	3.2	180.0	0.0013
0.9	50.4	0.0061	2.1	180.0	0.0056	3.3	173.0	0.0012
1.0	44.3	0.0060	2.2	180.0	0.0048	3.4	173.0	0.0011
1.1	39.5	0.0074	2.3	172.0	0.0045	3.5	180.0	0.0009
1.2	33.3	0.0073	2.4	180.0	0.0038			
The primary minimum θ_n along with corresponding $(d\sigma/d\Omega)_n$[a]								
1.8	14.4	0.0090	2.4	10.2	0.0092	3.0	7.9	0.0081
1.9	13.4	0.0091	2.5	9.7	0.0090	3.1	7.6	0.0078
2.0	12.6	0.0092	2.6	9.3	0.0087	3.2	7.4	0.0076
2.1	11.9	0.0093	2.7	8.9	0.0087	3.3	7.1	0.0074
2.2	11.3	0.0093	2.8	8.5	0.0085	3.4	6.9	0.0072
2.3	10.7	0.0093	2.9	8.2	0.0083	3.5	6.7	0.0070

[a]For incident momenta in the range [0.4,1.7] a.u. the critical angle lies upon the primary minimum. Beyond the incident momentum 1.7 a.u, though the critical angle shifts toward backward scattering angles, the primary minimum continues its forward movement.

In order to make an in-depth study of the critical points in elastic positron-hydrogen collisions we make use of surface plots. Various results for the elastic differential cross section are presented in Tables I–IV, and Figs. 1–17.

We find that for the incident momenta of positron below 0.3 a.u., the critical angle lies at the extremity of the backward direction of scattering (180°). This fact exhibits the dominance of the forward scattering over the backward scattering in this energy region. With the increase in incident momentum from just above 0.3 a.u., the critical angle (Figs. 1, 9, and 10, and Table I) begins to move in the forward direction to form the primary minimum. Subsequently the critical angle, lying upon the primary minimum, continues its forward movement with higher incident positron momentum. Further, when this incident momentum is just above 0.5 a.u. a secondary maximum begins to appear. With further increase in the incident momentum both the primary minimum and secondary maximum forming a certain wave pattern ap-

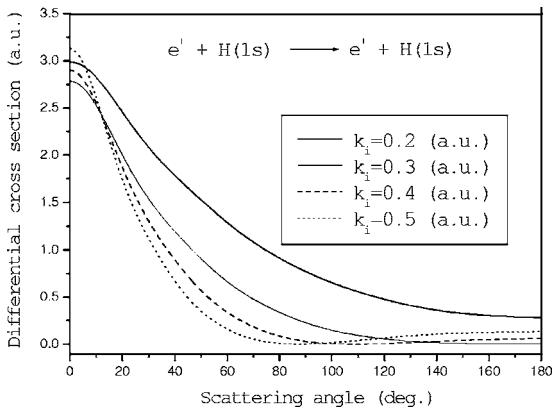

FIG. 1. The elastic differential cross section (a.u.) as a function of scattering angle θ^o (0°–180°) for the incident momenta k_i=0.2, 0.3, 0.4, and 0.5 a.u.

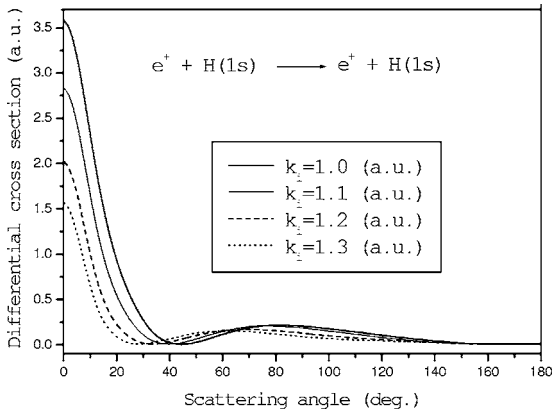

FIG. 2. The elastic differential cross section (a.u.) as a function of scattering angle θ^o (0°–180°) for the incident momenta k_i=1.0, 1.1, 1.2, and 1.3 a.u.

TABLE III. The successive partial-wave contribution to the elastic differential cross section (a.u.) in positron-hydrogen collisions as a function of scattering angle around the minimum for the incident positron momenta k_i=0.4,0.5 and 0.6 a.u..

k_i(a.u.)	Angle (deg)	l=0	l=1	l=2	l=3	l=4	l=5	l=6	l=7	l=8
0.4	106.2	0.09076	0.00818	0.00074	0.00060	0.00099	0.00032	0.00040	0.00065	0.00050
	106.7	0.09076	0.00707	0.00095	0.00046	0.00075	0.00021	0.00028	0.00047	0.00035
	107.2	0.09076	0.00606	0.00119	0.00034	0.00054	0.00015	0.00020	0.00033	0.00023
	107.7	0.09076	0.00512	0.00146	0.00025	0.00038	0.00012	0.00014	0.00022	0.00015
	108.2	0.09076	0.00426	0.00175	0.00017	0.00025	0.00012	0.00011	0.00014	0.00011
	108.7	0.09076	0.00349	0.00207	0.00012	0.00015	0.00016	0.00010	0.00010	0.00010
	109.2	0.09076	0.00279	0.00242	0.00009	0.00010	0.00024	0.00012	0.00009	0.00012
	109.7	0.09076	0.00218	0.00279	0.00008	0.00008	0.00034	0.00017	0.00011	0.00018
	110.2	0.09076	0.00164	0.00318	0.00008	0.00009	0.00047	0.00024	0.00016	0.00027
	110.7	0.09076	0.00119	0.00358	0.00011	0.00014	0.00063	0.00033	0.00024	0.00039
	111.2	0.09076	0.00081	0.00401	0.00015	0.00022	0.00082	0.00045	0.00034	0.00053
0.5	84.8	0.01836	0.04244	0.00043	0.00013	0.00091	0.00155	0.00085	0.00058	0.00080
	85.3	0.01836	0.03970	0.00020	0.00018	0.00063	0.00111	0.00053	0.00034	0.00052
	85.8	0.01836	0.03704	0.00009	0.00030	0.00041	0.00076	0.00029	0.00018	0.00031
	86.3	0.01836	0.03448	0.00009	0.00047	0.00024	0.00047	0.00014	0.00009	0.00016
	86.8	0.01836	0.03201	0.00021	0.00070	0.00012	0.00026	0.00006	0.00006	0.00007
	87.3	0.01836	0.02963	0.00042	0.00098	0.00005	0.00011	0.00006	0.00010	0.00005
	87.8	0.01836	0.02734	0.00074	0.00131	0.00004	0.00004	0.00014	0.00019	0.00007
	88.3	0.01836	0.02514	0.00116	0.00168	0.00007	0.00003	0.00028	0.00035	0.00016
	88.8	0.01836	0.02304	0.00167	0.00210	0.00015	0.00010	0.00050	0.00056	0.00030
	89.3	0.01836	0.02102	0.00228	0.00256	0.00027	0.00023	0.00078	0.00082	0.00050
	89.8	0.01836	0.01910	0.00297	0.00306	0.00044	0.00042	0.00112	0.00114	0.00074
0.6	71.2	0.00016	0.06679	0.00815	0.00081	0.00090	0.00220	0.00294	0.00233	0.00178
	71.7	0.00016	0.06356	0.00645	0.00064	0.00069	0.00164	0.00220	0.00166	0.00125
	72.2	0.00016	0.06041	0.00496	0.00062	0.00058	0.00119	0.00158	0.00114	0.00086
	72.7	0.00016	0.05733	0.00369	0.00076	0.00057	0.00084	0.00109	0.00076	0.00060
	73.2	0.00016	0.05432	0.00262	0.00105	0.00067	0.00059	0.00073	0.00053	0.00048
	73.7	0.00016	0.05139	0.00177	0.00148	0.00086	0.00044	0.00050	0.00043	0.00048
	74.2	0.00016	0.04853	0.00111	0.00205	0.00114	0.00039	0.00038	0.00046	0.00060
	74.7	0.00016	0.04574	0.00065	0.00274	0.00151	0.00043	0.00039	0.00063	0.00083
	75.2	0.00016	0.04303	0.00038	0.00355	0.00196	0.00057	0.00051	0.00092	0.00117
	75.7	0.00016	0.04040	0.00029	0.00447	0.00248	0.00079	0.00075	0.00133	0.00161
	76.2	0.00016	0.03785	0.00039	0.00550	0.00308	0.00110	0.00110	0.00185	0.00215

pear to be prominent (Figs. 2 and 11). The wrinkles in the surface plot of Fig. 14 clearly demonstrate this fact.

Some curves of $d\sigma/d\Omega$ are also shown in Figs. 3–5 to gain a deeper understanding.

The critical angle and primary minimum along with their corresponding differential cross sections are shown in Table II in the energy range 0.1–3.5 a.u. Further, an analysis of the numbers in Table I reveals an interesting fact. At higher incident positron energies, besides the primary minimum and secondary maximum, several local maxima and minima happen to occur one after another from the backward scattering direction.

In order to get a clear insight into this fact we have plotted the values of the differential cross section for the angles beyond 120° in Figs. 15, 16, and 17. As a matter of fact these local maxima and minima increase in number with increase in incident positron energy. Pushing the primary minimum in the forward direction, they emerge prominently, forming a regular wave pattern. This nature is very transparent from the surface plot Fig. 15. From Figs. 16 and 17 it is also clear that there exists a definite phase lag in the wave trains for different energies. Moreover, Table II shows that a global minimum of the differential cross section occurs at an incident momentum around 0.5 a.u. and at an angle around 87.3°. Thus the incident positron energy 3.4 eV corresponding to momentum 0.5 a.u. is the critical energy and 87.3° is the critical angle in elastic positron-hydrogen collisions in the energy range 0.1–3.5 a.u.. We observe from Table II that the chances of elastic scattering occuring at this point nearly vanish. Since at this particular positron momentum (0.5 a.u.) only elastic scattering can take place, therefore positron-

TABLE IV. The successive partial-wave contribution to the elastic differential cross section (a.u.) in positron-hydrogen collisions as a function of scattering angle around the maximum for the incident positron momenta k_i=2.7,2.8 and 2.9 a.u..

k_i(a.u.)	Angle (deg)	l=0	l=1	l=24	l=25	l=26	l=27	l=28	l=29
2.7	20.9	0.02190	0.08938	0.19518	0.19700	0.19935	0.20184	0.20416	0.20602
	21.4	0.02190	0.08907	0.19928	0.20159	0.20421	0.20675	0.20889	0.21041
	21.9	0.02190	0.08876	0.20303	0.20570	0.20846	0.21089	0.21273	0.21380
	22.4	0.02190	0.08844	0.20639	0.20929	0.21202	0.21422	0.21563	0.21618
	22.9	0.02190	0.08811	0.20930	0.21229	0.21485	0.21667	0.21758	0.21758
	23.4	0.02190	0.08778	0.21172	0.21465	0.21690	0.21824	0.21859	0.21805
	23.9	0.02190	0.08744	0.21360	0.21632	0.21814	0.21893	0.21871	0.21767
	24.4	0.02190	0.08710	0.21490	0.21727	0.21857	0.21877	0.21800	0.21655
	24.9	0.02190	0.08675	0.21559	0.21749	0.21821	0.21782	0.21656	0.21480
	25.4	0.02190	0.08639	0.21563	0.21698	0.21710	0.21616	0.21450	0.21256
	25.9	0.02190	0.08603	0.21504	0.21578	0.21529	0.21387	0.21194	0.20994
k_i(a.u.)	Angle (deg)	l=0	l=1	l=25	l=26	l=27	l=28	l=29	l=30
2.8	20.1	0.02029	0.08604	0.19733	0.19909	0.20134	0.20376	0.20603	0.20792
	20.6	0.02029	0.08576	0.20178	0.20403	0.20656	0.20905	0.21118	0.21274
	21.1	0.02029	0.08546	0.20585	0.20846	0.21113	0.21352	0.21536	0.21649
	21.6	0.02029	0.08516	0.20947	0.21230	0.21496	0.21710	0.21853	0.21914
	22.1	0.02029	0.08485	0.21259	0.21550	0.21798	0.21974	0.22066	0.22071
	22.6	0.02029	0.08454	0.21516	0.21798	0.22013	0.22142	0.22176	0.22127
	23.1	0.02029	0.08422	0.21712	0.21969	0.22140	0.22212	0.22189	0.22089
	23.6	0.02029	0.08390	0.21842	0.22061	0.22178	0.22191	0.22113	0.21970
	24.1	0.02029	0.08357	0.21902	0.22072	0.22129	0.22083	0.21956	0.21782
	24.6	0.02029	0.08323	0.21890	0.22003	0.21998	0.21897	0.21731	0.21540
	25.1	0.02029	0.08289	0.21807	0.21857	0.21793	0.21645	0.21452	0.21257
k_i(a.u.)	Angle (deg)	l=0	l=1	l=26	l=27	l=28	l=29	l=30	l=31
2.9	19.4	0.01885	0.08274	0.20019	0.20193	0.20412	0.20648	0.20872	0.21060
	19.9	0.01885	0.08247	0.20493	0.20715	0.20963	0.21206	0.21416	0.21573
	20.4	0.01885	0.08220	0.20924	0.21182	0.21443	0.21676	0.21857	0.21970
	20.9	0.01885	0.08191	0.21307	0.21584	0.21842	0.22049	0.22188	0.22250
	21.4	0.01885	0.08162	0.21633	0.21915	0.22152	0.22321	0.22408	0.22413
	21.9	0.01885	0.08133	0.21897	0.22166	0.22369	0.22487	0.22516	0.22466
	22.4	0.01885	0.08103	0.22092	0.22333	0.22489	0.22549	0.22520	0.22419
	22.9	0.01885	0.08072	0.22213	0.22412	0.22511	0.22511	0.22427	0.22284
	23.4	0.01885	0.08041	0.22256	0.22402	0.22440	0.22381	0.22249	0.22076
	23.9	0.01885	0.08009	0.22220	0.22305	0.22281	0.22168	0.22000	0.21810
	24.4	0.01885	0.07976	0.22105	0.22126	0.22043	0.21886	0.21693	0.21503

hydrogen scattering is nearly impossible in a direction of 87.3°.

The present findings indicate that interferences among the scattered waves of different angular momentum states produced by the interaction between the incoming positron and the target hydrogen atom are responsible for such dramatic behavior of the differential cross section. As an explanation we enlist the values of $d\sigma/d\Omega$ in Table III for the first nine partial waves around a critical angle (87.3°) at a critical energy (0.5 a.u.) to show how destructively they interfere at this point to produce the primary minimum. A secondary maximum is similarly found to be formed by a constructive interference of the scattered waves (as tabulated in Table IV). But, interestingly, the nature of formation of the primary minimum and secondary maximum are rather different. For the case of the primary minimum the states of lower angular momentum destructively interfere to produce such a picture whereas the states of higher angular momentum constructively interfere to produce such a hump. Away from the primary minimum and secondary maximum, the effect of interference between large-angular-momentum states produces an almost regular wave form. From this nature of the differential cross section one can get a deeper insight into the interaction during collisions.

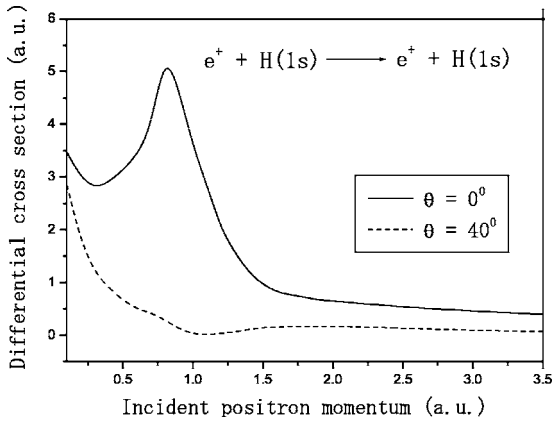

FIG. 3. The elastic differential cross section (a.u.) as a function of incident positron momentum k_i (0.1–3.5 a.u.) for the scattering angles θ=0° and 40°.

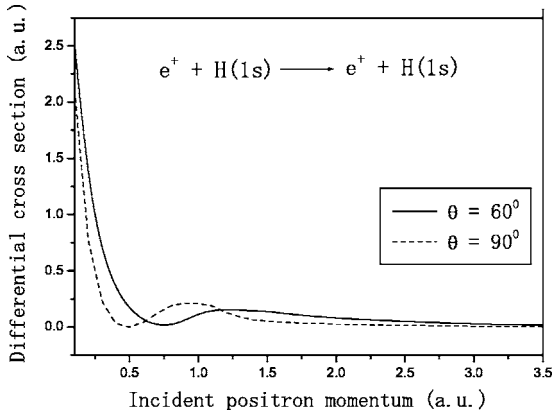

FIG. 4. The elastic differential cross section (a.u.) as a function of incident positron momentum k_i (0.1–3.5 a.u.) for the scattering angles θ=60° and 90°.

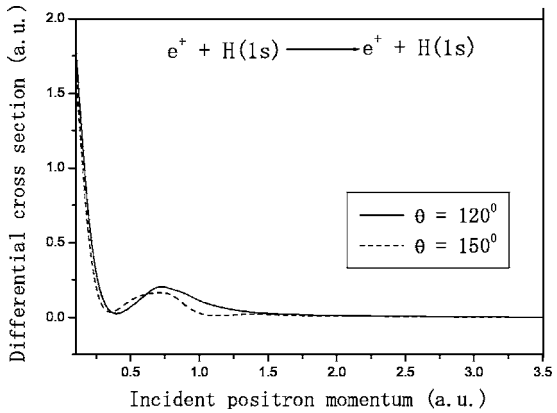

FIG. 5. The elastic differential cross section (a.u.) as a function of incident positron momentum k_i (0.1–3.5 a.u.) for the scattering angles θ=120° and 150°.

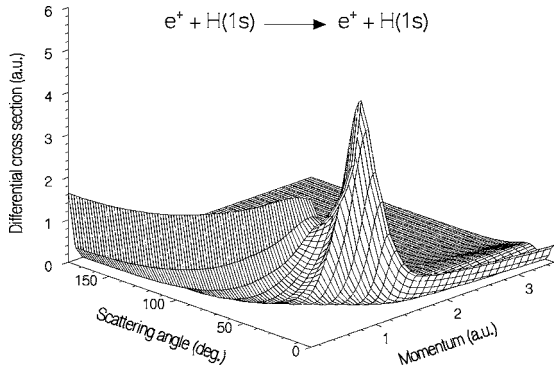

FIG. 6. The elastic differential cross section (a.u.) as a function of incident momentum k_i (0.1–3.5 a.u.) and the scattering angle θ (0°–180°).

Thus a comprehensive study seems to have been made on the elastic differential cross section for positron-hydrogen collisions at low and intermediate energies. Our investigations reveal the following detailed important information regarding the elastic differential cross section.

(i) Forward movement of the critical angle starts just beyond the incident energy of 0.3 a.u. This movement still continues around 15.7° (at an incident energy around 1.7 a.u.) where the differential cross section forms the primary minimum, and beyond this incident energy the critical angle makes a jump to 180° and becomes fluctuating.

(ii) Though the forward differential cross section is highly peaked there also exist secondary maxima besides the primary minimum.

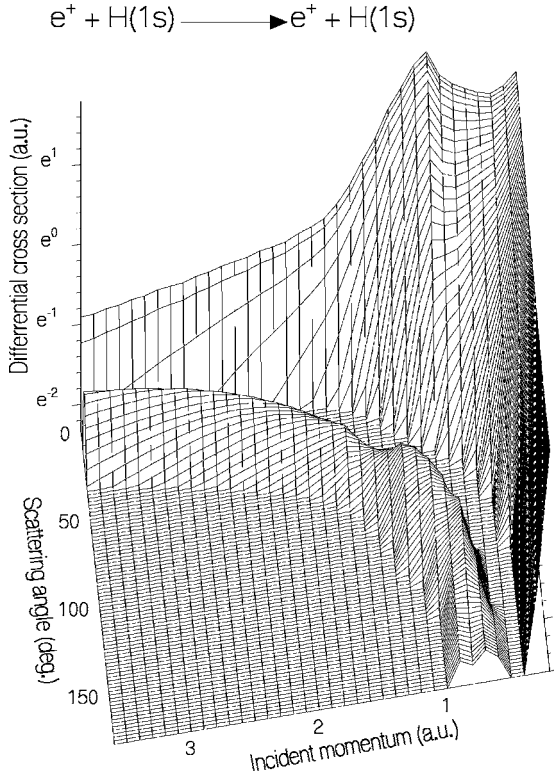

FIG. 7. The elastic differential cross section (a.u.) as a function of incident momentum k_i (0.1–3.5 a.u.) and the scattering angle θ (0°–180°).

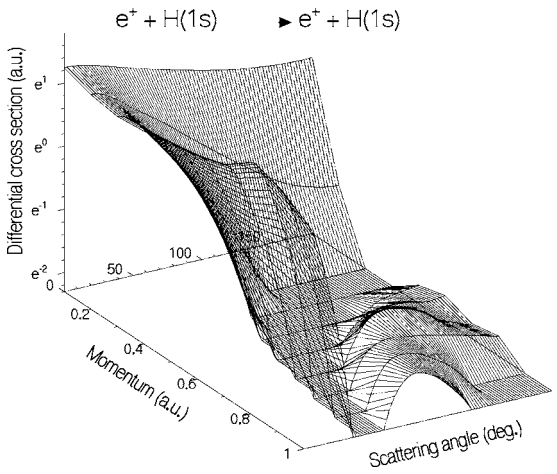

FIG. 8. The elastic differential cross section (a.u.) as a function of incident momentum k_i (0.1–1.0 a.u.) and the scattering angle θ (0°–180°).

(iii) Positron-hydrogen collisions nearly do not occur at the preferential incident positron momentum around 0.5 a.u. in around the 87.3° scattering direction.

(iv) The curve of the differential cross section assumes a wave pattern at large scattering angles beyond the incident positron energy of 3.4 eV for momentum 0.5 a.u. This wave pattern becomes prominent with increasing positron energy, and further there exists a definite phase lag between the curves of differential cross section for different incident energies.

(v) The interference of the scattered waves for different angular momentum states produced by the interaction between the incoming positron and the target hydrogen atom builds up the nature of the differential cross section.

(vi) The surface plots of the differential cross section display immensely rich structures.

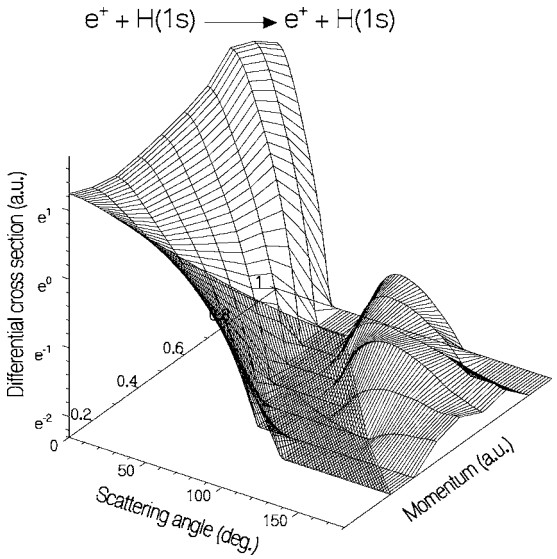

FIG. 9. The elastic differential cross section (a.u.) as a function of incident momentum k_i (0.1–1.0 a.u.) and the scattering angle θ (0°–180°).

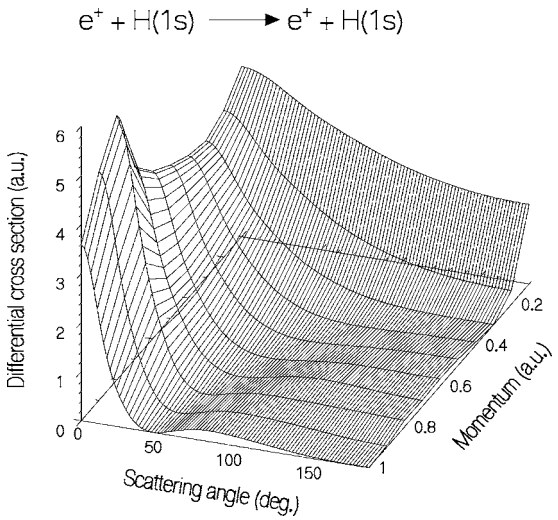

FIG. 10. The elastic differential cross section (a.u.) as a function of incident momentum k_i (0.1–1.0 a.u.) and the scattering angle θ (0°–180°).

IV. CONCLUSIONS

With the use of the phase shifts as obtained in paper I [1], in this work we have shown the manifestations of the nature of the elastic differential cross section, displaying rich structures.

The differential cross section for elastic positron-hydrogen collisions presents some hitherto unseen structures. The nature of the differential cross section is characterized by the existence and behavior of the critical points. Though the differential cross section is highly peaked in the forward direction, the forward movement of the critical angle with incident energy produces the primary minimum and second-

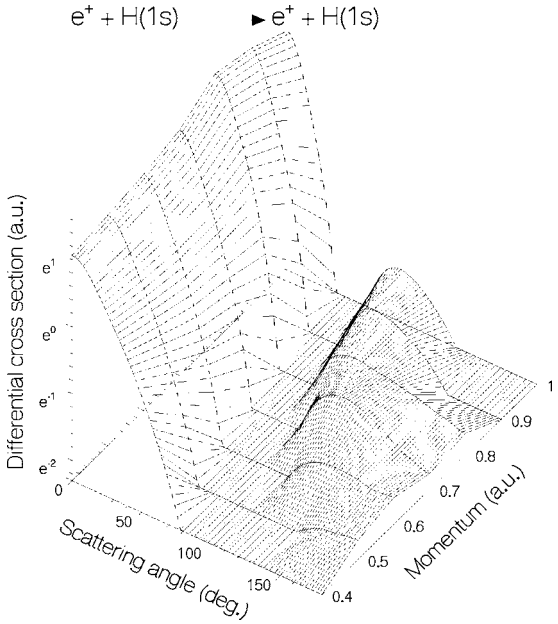

FIG. 11. The elastic differential cross section (a.u.) as a function of incident momentum k_i (0.4–1.0 a.u.) and the scattering angle θ (0°–180°).

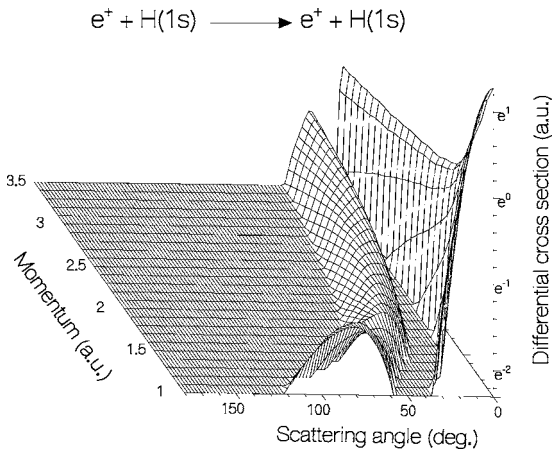

FIG. 12. The elastic differential cross section (a.u.) as a function of incident momentum k_i (1.0–3.5 a.u.) and the scattering angle θ (0°–180°).

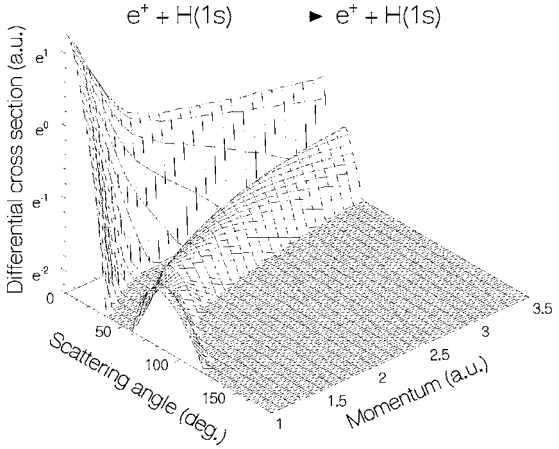

FIG. 13. The elastic differential cross section (a.u.) as a function of incident momentum k_i (1.0–3.5 a.u.) and the scattering angle θ (0°–180°).

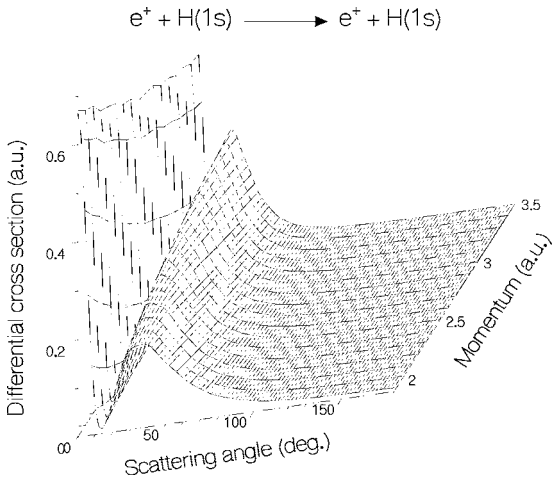

FIG. 14. The elastic differential cross section (a.u.) as a function of incident momentum k_i (1.9–3.5 a.u.) and the scattering angle θ (0°–180°).

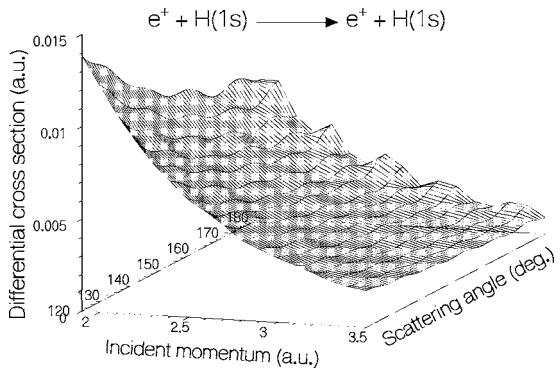

FIG. 15. The elastic differential cross section (a.u.) as a function of incident momentum k_i (1.9–3.5 a.u.) and the scattering angle θ (120°–180°).

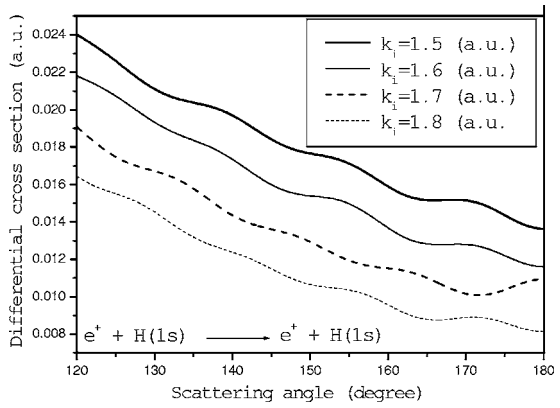

FIG. 16. The elastic differential cross section (a.u.) as a function of scattering angle θ (120°–180°) for the incident momenta k_i (1.5–1.8 a.u.).

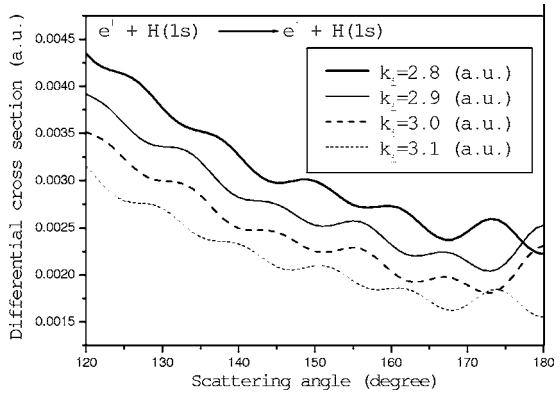

FIG. 17. The elastic differential cross section (a.u.) as a function of scattering angle θ (120°–180°) for the incident momenta k_i (2.8–3.1 a.u.).

ary maxima at intermediate and large scattering angles. It is found that interference of scattered waves of different angular momentum states is responsible for this nature of the differential cross section. On the one side destructive interference of the scattered waves of lower-angular-momentum states produces the primary minimum, while on the other hand, constructive interference of the scattered waves of higher-angular-momentum states produces a secondary maximum. Further, systematic constructive and destructive interference produces a regular wave pattern in the structure of the differential cross section at large scattering angles. Finally, the present findings reveal the remarkable fact that the positron-hydrogen scattering almost does not occur in the direction around 87.3° at an incident energy of about 3.4 eV corresponding to the incident positron momentum of 0.5 a.u.

ACKNOWLEDGMENT

A.G. wishes to thank University Grants Commission (UGC), New Delhi for financial support through a Minor Research Project [Grant No. F. PSW-006/03-04 (ERO)].

[1] A. Ghoshal and P. Mandal, Phys. Rev. A **72**, 042709 (2005).
[2] J. M. Wadehra, T. S. Stein, and W. E. Kauppila, Phys. Rev. A **29**, 2912 (1984).
[3] W. Buhring, Z. Phys. **208**, 286 (1986).
[4] P. Mandal, S. Kar, and U. Roy, Nucl. Instrum. Methods Phys. Res. B **143**, 32 (1998); Indian J. Phys., B **73**, 215 (1999).
[5] T. F. O'Malley, L. Spruch, and L. Rosenberg, J. Math. Phys. **2**, 491 (1961); Phys. Rev. **125**, 1300 (1962).